Materials and Design 160 (2018) 108–118

Contents lists available at ScienceDirect

Materials and Design

journal homepage: www.elsevier.com/locate/matdes

Responsive cellulose-hydrogel composite ink for 4D printing

Manu C. Mulakkal [a,*], Richard S. Trask [b], Valeska P. Ting [a,c], Annela M. Seddon [d,e]

[a] Advanced Composites Centre for Innovation and Science (ACCIS), University of Bristol, Queen's Building, University Walk, Bristol BS8 1TR, UK
[b] Department of Mechanical Engineering, University of Bath, Bath BA2 7AY, UK
[c] Department of Mechanical Engineering, University of Bristol, Bristol BS8 1TR, UK
[d] School of Physics, HH Wills Physics Laboratory, Tyndall Avenue, University of Bristol, Bristol BS8 1TL, UK
[e] Bristol Centre for Functional Nanomaterials, HH Wills Physics Laboratory, Tyndall Avenue, University of Bristol, Bristol BS8 1TL, UK

HIGHLIGHTS

- A sustainable and cost-effective responsive ink was developed for 4D printing
- The ink contained a high total cellulose content and good dispersion of cellulose fibres within the hydrogel matrix
- Ideal 3D printing extrusion characteristics were enabled via incorporation of additives and optimised material formulation

GRAPHICAL ABSTRACT

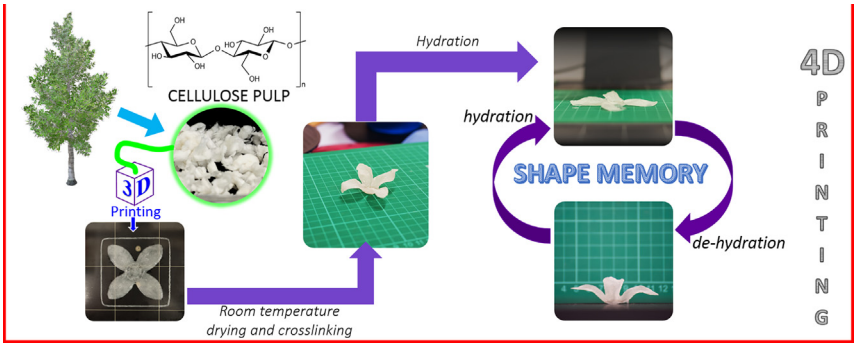

ARTICLE INFO

Article history:
Received 15 June 2018
Received in revised form 5 September 2018
Accepted 6 September 2018
Available online 7 September 2018

Keywords:
4D materials
Additive manufacturing
Composite morphing
Stimuli-responsive
Cellulose-hydrogel

ABSTRACT

Sustainable and cost-effective solutions are crucial for the widespread adoption of 4D printing technology. This paper focuses on the development of a cellulose-hydrogel composite ink for additive manufacture, presenting the development and physical characterisation (stability, swelling potential and rheology) of the cellulose-hydrogel composite to establish its suitability for 4D printing of responsive structures. The use of a carboxymethyl cellulose (CMC) hydrocolloid with incorporated cellulose pulp fibres resulted in an ink with a high total cellulose content (fibre volume fraction ≈50% for the dehydrated composite) and good dispersion of fibres within the hydrogel matrix. The composite ink formulation developed in this study permitted smooth extrusion using an open source 3D printer to achieve controlled material placement in 3D space while retaining the functionality of the cellulose. The addition of montmorillonite clay not only resulted in enhanced storage stability of the composite ink formulations but also had a beneficial effect on the extrusion characteristics. The ability to precisely apply the ink *via* 3D printing was demonstrated through fabrication of a complex structure capable of morphing according to pre-determined design rules in response to hydration/dehydration.

1. Introduction

With an increased focus on multifunctionality, the research community has been actively looking for new approaches for the development of responsive structures that can adapt to changes in their surroundings. While some approaches aim to achieve this *via* integration of complex sensory, electrical and mechanical systems with robotics and nanotechnology, some of the most elegant systems are based on smart structures that combine novel material chemistries with careful material placement. Many examples of "4D" structures (3D structures that can "morph" or change over time) already exist in nature [1]. For example,

* Corresponding author.
E-mail address: manu.mulakkal@bristol.ac.uk (M.C. Mulakkal).

https://doi.org/10.1016/j.matdes.2018.09.009

the hygroscopic unfolding response of pinecones (Fig. 1), the heliotropic sun tracking behaviour of various plants such as sunflowers and Cornish Mallow (*Lavatera cretica*) and the tactile response of 'touch-me-not' plants (*Mimosa pudica*) and various carnivorous plants are notable examples of structures that respond to an array of stimuli. These naturally responsive structures, relying on controlled arrangement of materials and simple responsive processes such as swelling, require no additional energy input to achieve the actuation [2]. Consequently there has been significant research effort and a large body of scientific literature [3–11] pertaining towards realising simple passive responsive systems analogous to those found in nature.

Following nature's design principles, two main requirements can be identified in order to realise such responsive systems: (i) a compliant stimuli responsive material and (ii) a process enables controlled placement of the compliant stimuli responsive material so as to achieve the desired response from the system (see the example in Fig. 1).

In terms of the first requirement, as a compliant stimuli-responsive material, the potential of cellulosic materials as precursors for cost-effective, renewable, bio-degradable and programmable smart materials has been previously demonstrated by the authors [12]. Cellulose, as the most abundant bio-macromolecule in nature, consists of β-1,4-linked anhydro-D-glucose units in which every unit is inverted 180° with respect to its adjacent units [13,14]. The presence of hydroxyl groups (OH) in the molecule (Fig. 2a) results in hydrogen bonding between molecules. This hydrogen bonding generates crystalline and amorphous phases within the cellulose structure [14] and leads to the formation of fibrils which further associate to form fibres in a true hierarchical fashion. Introduction of water to cellulose can result in plasticisation of the amorphous regions by weakening or relaxing hydrogen bonding through formation of competitive hydrogen bonds. These intercalating water molecules result in swelling throughout the material, which can be used to drive the reversible actuation of specific architectures created by these materials [12,15].

As a means to achieve the second requirement (controlled placement of the compliant stimuli responsive material), developments in additive manufacturing technology (3D printing) enable a high degree of control over the placement of materials in 3D space, thereby enabling the design of hybrid structures that have the hierarchical structural complexity characteristic of functional biological systems. Strain mismatch within a substrate is the driving force for many of the transformations in nature as well as for many synthetic actuators upon activation by the stimuli. Swelling is one of the simplest way to realise strain differential in a substrate. Combined with the morphing response of cellulose to stimulus (*e.g.* water), a time-dependant transformation of a printed 3D shape could be triggered, to produce a "4D" printed structure. This approach is analogous to the "4D printing" concepts developed and demonstrated at MIT [16], which utilise materials with shape memory and volumetric expansion properties to achieve micro to macroscopic actuation responses [17–20]. The use of 3D printing to achieve shear-alignment of cellulosic fibrils to preferentially control the swelling of an embedding matrix would further emulate the macroscopic response demonstrated in the hierarchical structure of natural 4D materials, such as the pinecones described above [2,21].

While cellulose, as a potential 4D printing feedstock, has benefits such as environmental friendliness, biodegradability and low cost [22–24], in its native form, cellulose is not compatible with current commercial 3D printing/additive layer manufacturing systems as it cannot be melted and extruded in a similar manner to existing 3D printing polymer feedstocks, nor sintered with a laser, such as is commonly done with ceramic/metal/polymer beads. Commercial 3D printing filaments comprised of cellulosic materials systems do exist where the cellulose is in the form of sawdust or recycled wood forming fillers (≈30%) hosted within a polymer matrix such as PLA (polylactic acid) [25,26]. However, this method limits the exposure of cellulosic components to the environment/stimuli and hence such approaches are not appropriate for 4D morphing applications. Markstedt et al. 3D printed cellulose by dissolving three different types of cellulose (namely bacterial nanocellulose, Avicel-PH-1-1 and dissolving pulp) in ionic liquids (IL) followed by coagulation, resulting in 2D and multilayer 3D gel structures on a coagulating bed, allowing ionic solutions with cellulose

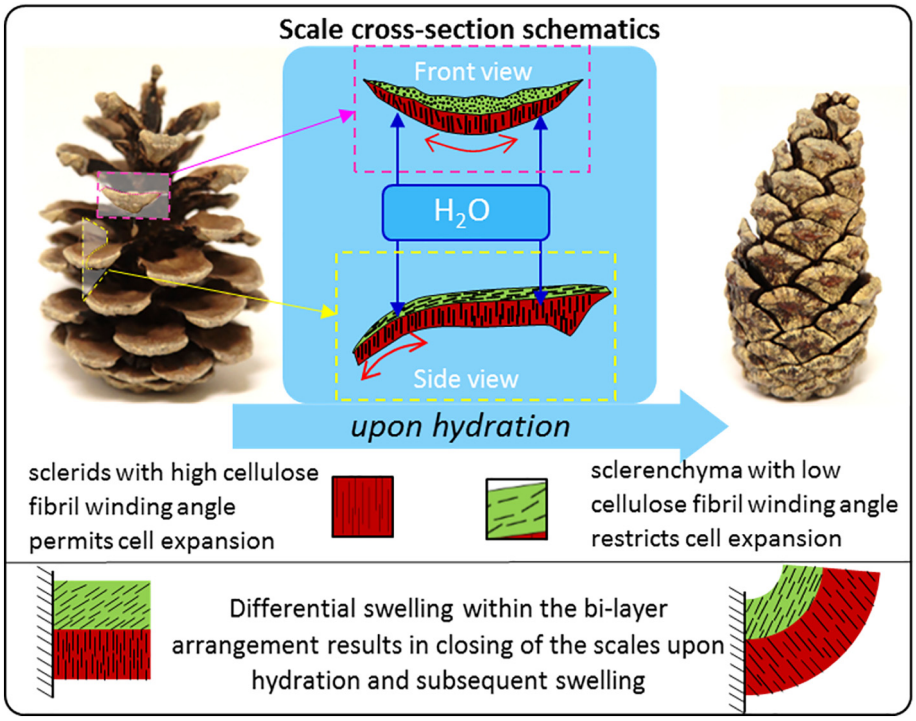

Fig. 1. Stimulus-response of pine cones. (left) Dehydrated open pinecone; (right) hydrated closed pinecone; Differences in the cellulose fibril winding angles in the top and bottom layers of the cells (sclerids in red and sclerenchyma in green) control the expansion of these cells during hydration/dehydration. The cooperative anisotropic expansion of these differentiated cells result in the opening and closing of pinecone scales in response to hydration.

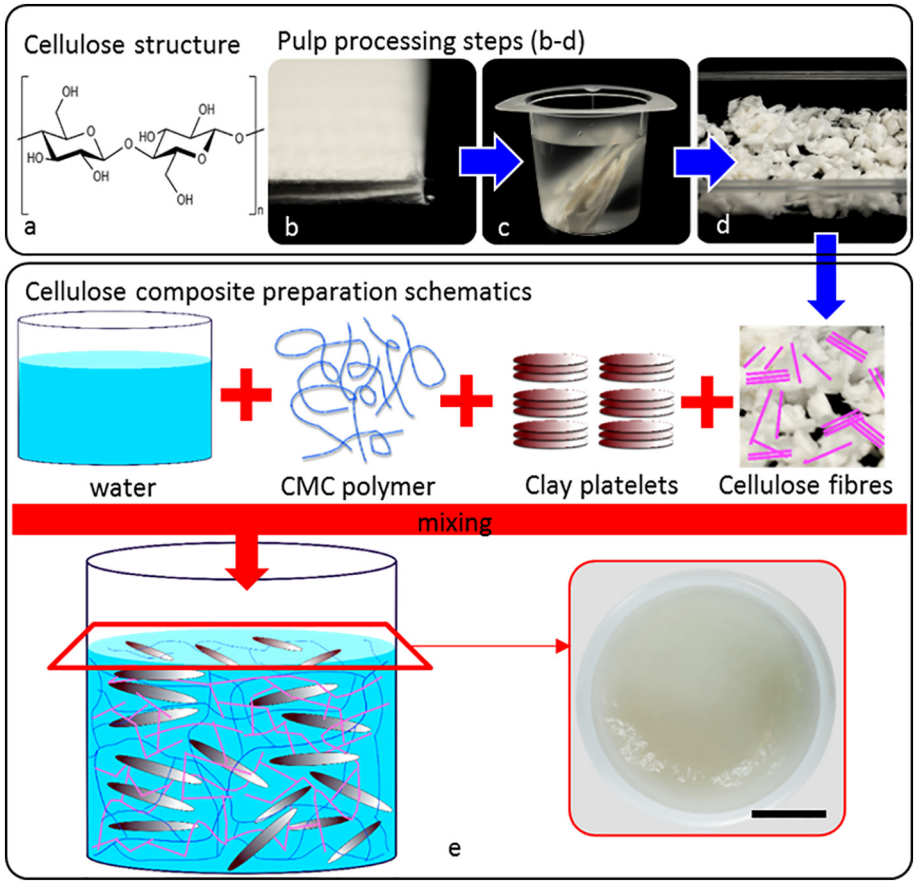

Fig. 2. (top) (a) Structure of cellulose. (b–d) Processing of cellulose fibres from pulp linters (b) Pressed pulp linters as received (c) pieces of pulp linters saturating in reagent grade water prior to breaking up and (d) pulp in the process of drying at room temperature. (bottom) (e) Schematics of the preparation of hydrogel-composite and the final mix shown in insert (Scale bar: 20 mm).

concentrations of 1%, 2% and 4% to be 3D printed [27]. Composite bio-inks have also been prepared by combining cellulose nanofibril (NFC) dispersions in an alginate-based hydrogel consisting of 95–99% water, crosslinked by immersion in calcium chloride ($CaCl_2$) solution [28]. However, the cellulosic content of the reported bio-ink was very modest (1.5%–2.3% w/v). Hakansson et al. reported similar bio-inks where the 3D dry state shape was achieved by means of freeze drying the bio-ink print [29], with similar approaches in cellulose printing also being reported by researchers at Aalto University (Finland) and VTT research (Finland) as part of their joint DWOC (Design Driven Value Chains in the World of Cellulose) program [30]. Leppiniemi et al. reported a nanocellulose-alginate hydrogel with good tissue compatibility for 3D printing [31]. The nanocellulose content within printable hydrogel formulations varied from 0.5%–1.3% w/w. However, it should be noted that even though these approaches enabled 3D printing of cellulose, the focus was predominantly placed on tissue engineering applications. As such, the final shapes (achieved after drying) were fixed and the morphing behaviour of these material systems was not shown or investigated. A 3D structure containing cellulose nanofibrils (NFC) capable of transforming in the time domain as envisaged in 4D printing was recently demonstrated by Gladman et al. who fabricated plant-inspired architectures using NFC in acrylamide ink. These architectures actuated as a result of preferential swelling in an acrylamide gel when restricted by the shear alignment of NFC along the print path, with 0.8 wt% of NFC used as "stiff fillers" to prepare the composite ink [19]. Such research shows that adapting cellulosic materials to the 3D printing domain can be achieved but there is scope for discovery especially with regard to enabling 3D printing of smart materials with high cellulosic content, and to make better use of the hydration-response of the cellulose itself. In addition, the need for porosity and the resulting network structure of pulp fibres in controlling the opening and closing of folds in paper architectures has been previously established [12]. When used with 3D printing, the shear-alignment of the cellulosic fibrils would not only enhance the mechanical properties of the substrate but also provide additional parameters such as porosity and anisotropic stiffness which can be programmed to further tailor the response to stimuli.

While 3D printing in general is experiencing a widespread popularity thanks to low cost 3D printers empowered through open-source projects such as RepRap [32,33], the costs associated with 4D printing, including the novelty of the compliant materials and associated proprietary 3D printers renders most 4D printing technology prohibitively expensive and has hindered its extensive adoption and widespread implementation. Future advancement of 4D printing technology depends on the development of a greater variety of stimuli responsive smart materials that can be used in conjunction with 3D printing for precise control of material placement as well as a clear understanding of the design principles, to allow mathematical modelling and tailoring of the actuation response [18]. To address this, this paper focuses on the development of a cost-effective, compliant "ink" material that can enable 3D printing of stimuli responsive complex forms to create programmable 4D structures. Moreover, the cellulosic ink will be specifically tailored for 3D printing using low-cost, open-source 3D printers ensuring the cellulosic composites thus fabricated are able to be further developed and extensively adopted in 4D printing research.

In this work, we have developed a stimuli responsive cellulosic pulp-hydrogel composite ink that is cost effective and bio-degradable. This composite ink is formulated for 3D printing and the stability, rheology and swelling potential of the ink has been characterised. A functional complex shape was fabricated using 3D printing to achieve precise material placement of the cellulosic ink, and the actuation *via* exposure to

water demonstrated the ability to use this ink to produce 4D structures capable of programmable transformation.

2. Materials and methods

2.1. Materials selection and ink formulation

A range of cellulose-derived polymers that can form hydrogels exist [24,34] and the cellulose-derived polymer chosen for this study was sodium carboxymethyl cellulose (CMC-Na/CMC) as it was shown to be easily hydrated and exhibited self-healing properties [35]. CMC is a hydrophilic cellulose derivative with carboxymethyl groups bound to the hydroxyl groups of glucose. The functional properties of this biocompatible carbohydrate depend on its degree of substitution. The polar nature of carboxylic group makes CMC soluble in water resulting in the formation of gel. This polymer is widely used in food, skin care and the drug industry as a thickening agent/rheological modifier and is biocompatible.

Cotton derived pulp linters (fibres) such as those used in the paper making industry were selected as the cellulosic fibre component. These are recognised to have a high cellulose content (≈99%) and purity [36] though the purity of the supplied pulp fibres was not analytically assessed. Pressed cotton pulp linters for papermaking were obtained from *George Weil Art & Craft Supplies* (*www.georgeweil.com*). Optical microscopy analysis of the pulp linters revealed a highly compacted network of cellulose fibres with an average width of 14.2 ± 2.6 μm.

Reagent grade water from Fisher Scientific was used as-received. CMC-Na with degree of substitution (DS) of 0.9 in molecular weight (Mw) of 700 k and 250 k were obtained from Arcos Organics. Hydroxyethyl cellulose (HEC) was obtained from Merck Millipore. Montmorillonite (naturally occurring mineral) and citric acid (99%) were purchased from Alfa Aesar and Sigma Aldrich respectively. Polyacrylic acid (PAA) was purchased from Sigma Aldrich. All materials were used as supplied.

For uniform dispersion of pulp fibres in water, a planetary shear mixer (Thinky Mixer, USA) which employs "rotation" and "revolution" movements, was used for material mixing. The Thinky Mixer mixing procedure involved adding the pulp, water and CMC in small increments (≈15–20 wt% of total batch, 30 mL of water) and mixing for 30 s at 1600 rpm before adding further increments up to the required amount as per the recipe.

Clay (montmorillonite, 0.5 wt% of water) was added as a filler in order to stabilise the hydrogel. The montmorillonite platelets were exfoliated in water through adequate agitation. The storage stability of the gel and composite formulations containing clay and CMC was assessed by an inversion test carried out on one-week old samples in polypropylene vial of 28 mm in diameter and 115 mm in length.

The cellulose-hydrogel composites were manually extruded through a syringe (as in a 3D printer print head) of diameter ≈1 mm and dried to form thin films. Standard films (dry) of CMC polymer were left immersed in water overnight to test stability. Crosslinking reactions involving self-crosslinking [37], crosslinking with PAA (poly acrylic acid) [38,39] and citric acid (CA) [35,40,41] as crosslinking agents were carried out and evaluated by immersing in water overnight. The crosslinking reactions with citric acid were successfully completed *via* exposure to 120 °C for 10 min as opposed to 180 °C for 30 min for self-crosslinking and 140 °C for 30 min when PAA was used. Reaction parameters were obtained from the study of Demitri et al. [40] and adapted for the synthesis of hydrogel composites. A mixture of CMC-Na and HEC (hydroxyethyl cellulose), with weight ratio equal to 3:1 was used to form a hydrogel, with the HEC used to promote intermolecular rather than intramolecular crosslinking [40].

2.2. Characterisation of swelling ratio

The swelling response of the developed formulations was investigated *via* calculation of the equilibrium swelling ratio (SR) of dried and crosslinked formulations containing citric acid on immersion in de-ionised water. The samples (minimum of 3 repeats) were weighed and immersed in de-ionised water for 24 h to reach equilibrium swelling at room temperature (21 °C). The samples were recovered from water and weighed after removing excess water from the surface by gently patting with tissue paper.

The SR was calculated as follows:

$$SR = \left(\frac{W_s - W_d}{W_d}\right) \quad (1)$$

where W_s is the weight of the swollen hydrogel/composite, and W_d is the weight of the dried sample. The experiment to determine the swelling ratio of the formulations also provide additional insight into their aqueous stability.

2.3. Rheological characterisation

A series of amplitude sweeps (strain), frequency sweeps, steady-state shear tests and stress-ramp tests were carried out to characterise the rheological behaviour of the hydrogel and composites. A strain sweep from 0.01%–100% at a frequency of 1 Hz was performed on gelled samples. Frequency sweeps from 0.1 Hz–10 Hz were conducted on formed gel samples at 0.5% strain (within the linear visco-elastic regime (LVER)).

This protocol was adapted from [42,43]. A rheometer (Kinexus Pro) from Malvern Instruments with a parallel plate geometry (PU20) of diameter 20 mm was used and all the samples were tested at 25 °C. Each sample (≈1.5 mL) was used only once, and the tests were performed in triplicate and the error bars represents the corresponding standard deviation. A standard loading sequence was used to guarantee reliable and precise loading protocol.

2.4. 4D printing of cellulosic composites

The materials developed and characterised in this study enable extrusion through a syringe which is the proposed dispensing method for integrating with open-source 3D printing hardware. The rheometry results informed the selection of the extruder system (*i.e.* motor choices and power output), allowing the integration of this material system into a 3D printer. A custom off-axis direct driven paste extruder based on an open-source syringe extruder [44] was fabricated and integrated with a commercially available Prusa Mk2 3D printer. The choice of morphing petal architecture to validate the 3D printing capabilities and subsequent 4D morphing of the developed cellulose formulations was influenced by the familiarity of the petal architecture itself thereby establishing an equivalence with other methodologies and ink formulations which have used a similar shape to demonstrate responsiveness. The form was fabricated from a CAD model and prepared for 3D printing (sliced) within the MatterControl software with an infill of 99%. The substrate was printed from Composite + Clay + CA with an additional circular layer of Gel + CA at the base of the petals. A 0.8 mm tapered nozzle was used for printing with a layer height of approximately 0.6 mm. The drying of the specimen at room temperature (RT ≈ 21 °C) initiated the transformation which was maximised by crosslinking at 120 °C for 10 min fixing the new configuration. This transformed shape was rehydrated by placing in a water bath at room temperature (21 °C) in a similar fashion to that of the preceding work reported in [12].

3. Results and discussion

3.1. Ink formulation and processing

The process for preparing and processing of the cellulose-hydrogel composite ink formulations is summarised in Fig. 2. To achieve a balance between benefits of a fibrous network without compromising the gel nature, a 50% fibre V_f (volume fraction) of the final composite (*i.e.* half fibre - half CMC polymer) was selected.

The pulp linters were saturated in water for ≈24 h (Fig. 2 (top row) c), to disrupt the hydrogen bonding between individual fibres followed by manual agitation of the linters using a spatula, before drying at room temperature (Fig. 2 (top row) d). The uniform dispersion of pulp fibres in water is crucial for formation of a fibre suspension suitable for subsequent processing and smooth extrusion through syringe heads during printing. The extensive hydrogen bonding occurring at both the intermolecular and intramolecular levels in the cellulose pulp promote aggregation. To prevent this in a limited volume of water requires introduction of a shear force. Addition of CMC polymer not only served the function of bypassing the undesirable shear thickening by changing the nature of the material system (*i.e.* from suspension to a gel or paste) but also enabled effective transfer of shear forces to separate pulp fibres. Based on preliminary dispersion trials it was deemed that within a laboratory environment only a minimal volume of pulp fibres (significantly lower than the target V_f) could be evenly dispersed in a beaker before starting to compromise the gel nature of the composite as the addition of a greater volume of fibres to increase V_f inevitably required further addition of water to facilitate fibre dispersion. The gel nature is crucial to enable extrusion as suspensions tend to exhibit shear-thickening which hinders the flow under stress [45]. As such, a balance is required so as to maximise the fibre V_f without compromising the gel nature of the composite.

A general schematic of composite preparation is presented in Fig. 2 (bottom row). A number of mixing strategies were investigated ranging from sonication and shear mixing besides mechanical agitation with a spatula but yielded less than ideal results as evidenced by the fibre agglomeration observed in prepared films (Fig. 3a–c, showing large (up to ≈10 mm) clumps of fibres). However, adding a hydrocolloid such as CMC before and during the mixing of pulp in water showed some promise when extruded to form thin films (Fig. 3c). This strategy was further refined to yield improved extrusion results. The composition of the final hydrogel composite was 0.025 g each of pulp and CMC polymer per 1 mL of water. Fig. 3 illustrates the differences in pulp dispersion in the hydrogel composite using different mixing approaches, with the image in Fig. 3d clearly showing an absence of the large fibre clumps in the Fig. 3a, b and c, and a lack of large transparent regions in the prepared films (demonstrating areas of low cellulose fibre content). The best dispersion results (Fig. 3d) for this formulation were obtained with a planetary mixer, which employs “rotation” and “revolution” movements for material mixing. This resulted in the efficient shear transfer of centrifugal forces in separating and dispersing the pulp fibres facilitated by the addition of gel forming polymer to enable clog free extrusion. Once all the components were combined, the mixture was further blended for 3–4 min (depending on the total volume) to obtain a uniform paste (Fig. 2e, bottom row insert) to allow for smooth extrusion.

For usability of the composite ink in 3D printing, long-term structural stability of the gel was an important factor. It was noted that a significant reduction in the composite gelling properties and viscosity had occurred after a week despite being stored in a sealed container. Clearly, this is not an ideal feature as the materials then had to be prepared immediately prior to extrusion and lacked flexibility for storage for later use. Therefore, storage stability was deemed essential for the materials developed. Clay (montmorillonite) was added (0.5 wt% of water) as a filler in order to stabilise the hydrogel in this regard. Montmorillonite is a layered silicate with a lamellar structure and commonly used as an additive to improve the mechanical properties of polymers in general. Once exfoliated, the montmorillonite platelets can effectively intercalate between the polymer chains and fibres delaying the weakening of the gel and composite formulations. The schematic of this process is presented in Fig. 2 (bottom row). The exfoliation of the platelets in water is by virtue of layer separation brought about through hydration forces as well the hydration of the cations (Fe^{+}, Fe^{2+}, Mg^{2+} and Al^{3+}) present in montmorillonite [46]. An off-white colour was imparted to the hydrogel composite as a result of adding clay. The storage stability of gel and composite formulations containing clay and increased CMC was assessed by an inversion test. One-week old samples of composite formulations containing clay and increased molecular weight CMC (Mw 700,000) was assessed by an inversion test and demonstrated more stability in the inverted position in the container than formulations with low Mw CMC polymer devoid of clay. The molecular weight (Mw) of CMC used was thus increased from 250,000 to 700,000 to improve viscosity and stability.

For deployment of the hydrogel-based actuators, the stability in aqueous medium was also important to determine. Standard films (dry) of CMC polymer disintegrated (became soluble) in water when left immersed overnight. Films of cellulose-hydrogel composite retained their ‘shape’ in an aqueous medium overnight but disintegrated when handled, confirming that the pulp network alone is insufficient to retain structure during immersion. In order to provide aqueous stability, it was decided to crosslink the hydrogels. Crosslinking reactions involving different crosslinking agents were carried out and evaluated by immersing in water overnight. The crosslinking reactions with citric acid were successfully completed *via* exposure to 120 °C for 10 min as opposed to 180 °C for 30 min for self-crosslinking and 140 °C for 30 min when PAA was used. A mixture of CMC-Na and HEC (hydroxyethyl cellulose), with weight ratio equal to 3:1 was used to form a hydrogel, with the HEC used to promote intermolecular rather than intramolecular crosslinking [40]. As a result of the testing, the formulations containing 10% (of total polymer content) CA was chosen for the milder reaction conditions and taken forward for further evaluation. Once the composition of the cellulose-hydrogel composite had been decided upon, a range

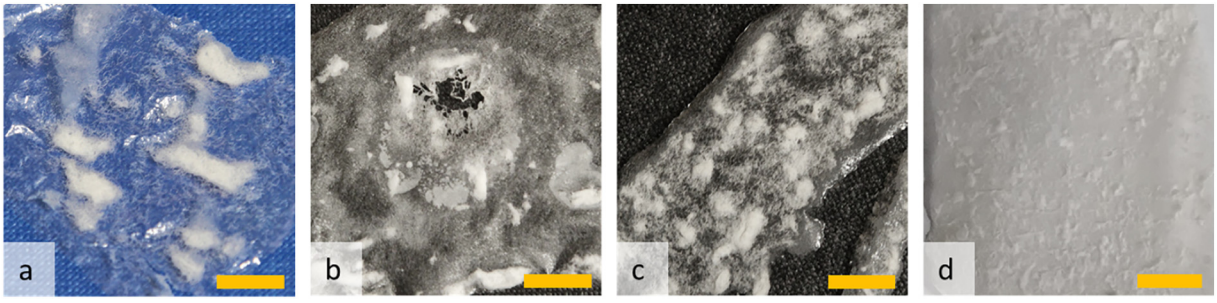

Fig. 3. Pulp-CMC composite films illustrating the improvements in pulp dispersion as a result of optimised mixing strategies: (a) mechanical agitation with spatula (b) ultra-sonication (c) shear mixer and (d) non-contact planetary shear mixer (Scale bar: 10 mm).

of formulations were produced and used for the testing, as detailed in Table 1.

Gel + CA (low) has the same polymer content (2.5 wt% of total water content) as the composite samples and the polymer content in the other two gel samples is equivalent in weight to the solid (polymers and pulp) content of the composite samples (5 wt% of total water content). This spectrum of samples would demonstrate the effect of pulp, clay and polymers forming the gel in governing the rheological characteristics of these samples.

3.2. Characterisation of swelling ratio

The aqueous stability and swelling capacity of the formulations were assessed by calculation of the equilibrium swelling ratio and the results are summarised in Table 2. The standard deviation is presented as the uncertainty. The swelling ratios of comparable self-crosslinked samples (without citric acid) are also presented to better understand the effect of crosslinking agent and to demonstrate the possibility of programming the swelling response by varying the amount of crosslinking agent. The effectiveness of citric acid in crosslinking at relatively lower temperature is clear when compared to self-crosslinked samples. The effect of pulp fibres on the swelling ratio is also evident. This confirms the presence of a pulp network that restricts the swelling of hydrogel matrix resulting in a lower swelling ratio. The addition of montmorillonite clay was found to have no impact on swelling ratio. In swelling-induced shape transformations, the equilibrium swelling ratio results presented might come across as an apparent limitation as they are significantly lower than for the self-crosslinked samples. However, what is more significant is the ability to realise the strain gradient in substrates in a controlled manner. The versatility of this approach is that the amount of crosslinking agent or the ratio of cellulosic polymers (CMC: HEC) can be varied so as to achieve desirable swelling specific for a structure.

3.3. Rheological characterisation

The formulations with citric acid as a crosslinking agent were subjected to full characterisation *via* rheological testing, to determine the mechanical properties of the hydrogel and associated composites. The gelation times were not determined using rheological parameters as the gel formation with CMC was observed as a function of loading capacity and consistently resulted in the formation of gels during the synthesis step for the formulations investigated (see Table 1). The effect of amplitude, frequency and shear rate on elastic (storage) modulus G′ (representing the solid-like characteristics of the samples) and viscous (loss) modulus G″ (representing the liquid-like characteristics) were used as an indication of the nature and flow characteristics of the samples. The relative importance of G′ and G″ is represented by phase angle (δ) as follows:

$$\tan(\delta) = \frac{G''}{G'} \tag{2}$$

when δ > 45° (*i.e.* G″/G′ > 1), it can be said that liquid-like behaviour dominates within the sample.

Table 1
Sample nomenclature and respective formulations.

Sample name	Key - water/gel polymer/pulp/clay/cross-linker (in grams)
Gel + CA (low)	$30_{\text{water}}/0.75_{\text{polymer}}/0_{\text{cellulose}}/0_{\text{clay}}/0.15_{\text{cross-linker}}$
Gel + CA	$30_{\text{water}}/1.5_{\text{polymer}}/0_{\text{cellulose}}/0_{\text{clay}}/0.15_{\text{cross-linker}}$
Gel + Clay + CA	$30_{\text{water}}/1.5_{\text{polymer}}/0_{\text{cellulose}}/0.15_{\text{clay}}/0.15_{\text{cross-linker}}$
Composite + CA	$30_{\text{water}}/0.75_{\text{polymer}}/0.75_{\text{cellulose}}/0_{\text{clay}}/0.15_{\text{cross-linker}}$
Composite + Clay + CA	$30_{\text{water}}/0.75_{\text{polymer}}/0.75_{\text{cellulose}}/0.15_{\text{clay}}/0.15_{\text{cross-linker}}$

Table 2
Equilibrium swelling ratio of formulations with citric acid (CA) after crosslinking.

Crosslinked with CA	10 min at 120 °C	Self-crosslinked	30 min at 180 °C
Gel + CA	2.6 ± 0.2	Gel	38.3 ± 1
Gel + Clay + CA	2.8 ± 0.1		
Gel + CA (low)	1.4 ± 0.3		
Composite + CA	0.85 ± 0.02	Composite	4.1 ± 0.1
Composite + Clay + CA	0.82 ± 0.03	Composite + Clay	6.2 ± 0.2

3.4. Strain sweeps

Fig. 4 shows the elastic modulus (G′) and phase angle (δ) as a function of shear strain for the samples tested. The loss modulus (G″) values were not included for clarity but are embodied in the phase angle (δ) data presented. The phase angle (δ) data also demonstrates that G′ > G″ (δ < 45°) for most of the applied strain regime indicating that the samples are structured (gel). Elastic modulus values measured within the LVER (linear visco-elastic regime) shows the highest value for Gel + Clay + CA (1.15 kPa) samples, as expected. The presence of clay results in a higher elastic modulus and viscosity when compared to Gel + CA (0.9 kPa) samples. Contrary to what was observed in gel samples, the addition of clay in composites did not increase the elastic modulus (≈0.7 kPa) but resulted in gradual decay of modulus and viscosity at lower strains followed by a rapid decay of modulus which signified the critical strain %. The onset of non-linearity is termed as critical strain % and the gel structure is disrupted when strain values exceed beyond this point. It is assumed that the structural interactions of intercalated clay and dispersed pulp fibres resulted in this flow behaviour. As the sampled gels were not chemically crosslinked, the gel nature was by virtue of physical crosslinks such as hydrogen bonding. Montmorillonite is of layered structure and could reduce the effective hydrogen bonding between cellulosic pulp, polymers and water by intercalating between them. This is reflected in the δ data as a rapid rate of increase in phase angle indicate more fluid like behaviour under increasing applied strain. Although further investigations as to why this behaviour arises are necessary, these characteristics are ideal for the proposed composite extrusion system as it not only provides long term stability to the material system but also the composite gel containing the clay flows more easily when compared to other formulations in this study. It is also noted that the modulus and thus the δ data for Gel + CA (low) are particularly noisy at strain (0.01%–0.1%) as expected due to weaker response at this strain range from the sample.

3.5. Frequency sweeps

Frequency sweeps from 0.1 Hz–10 Hz were conducted on formed gel samples at 0.5% strain (within the LVER) with the results of the frequency sweeps presented in Fig. 5. The results represent the G′ variation and phase angle (δ) across the probed frequency range. Loss Modulus (G″) values were omitted for clarity and relative significance of elastic and viscous modulus is presented as phase angle dependence on frequency. It can be seen that the elastic modulus values at 1 Hz matches the G′ values in the LVER regime for the amplitude sweep results presented in Fig. 4. The recorded response in G′ suggests that the modulus is dependent on the frequencies probed and implies some structural relaxation where stored elastic energy is dissipated with time. There is no crossover point for the modulus as evidenced by δ values < 45° within the designated frequency range. However, analysis of the phase angle (δ) trends in Fig. 5 implies possible crossover frequencies ≪ 0.1. The precise crossover frequencies and thus relaxation times were not determined due to time-related impracticalities in running scans at such low frequency levels. The phase angle δ data also shows G′ > G″ validating the presence of structured gel as observed in the amplitude sweep results.

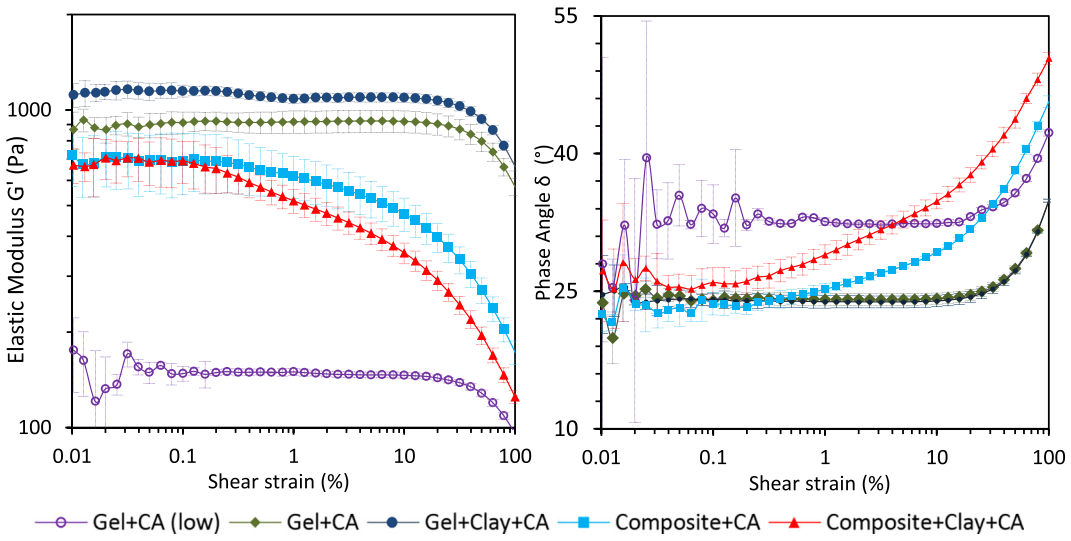

Fig. 4. Amplitude sweep data showing elastic modulus (G′) (Log scale) and phase angle (δ) as the function of shear strain.

3.6. Shear rate

The results of the steady state shear measurement are presented in Fig. 6, as viscosity and shear stress as a function of shear rate. It can be seen that the samples are highly shear thinning from the shear viscosity–shear rate response confirming pseudoplastic behaviour as expected. The relationship between shear stress developed and the applied shear rate is also presented. It can also be observed that the viscosity and stresses of Composite + Clay + CA samples are closer to the Gel + CA (low) samples especially at higher shear rates (representing short times) even though the solid content within the specimen is twice as high. This underlines the suitability of the Composite + Clay + CA sample for short time processes such as extrusion. The comparison of viscosity and shear stress developed in Composite + Clay + CA, Gel + CA and Gel + Clay + CA confirms the observation made in amplitude sweep analysis regarding the combined effect of pulp and clay in facilitating better extrusion. These results show the effectiveness of pulp-gel composite system in having ideal extrusion characteristics for 3D printing as a homogenous phase of either of the two would not have yielded necessary high viscosity (solid-like) at rest and decreasing at higher shear rates (*i.e.* when deformed).

3.7. Stress ramp

Yield stress signifies the stress required to break the physical interactions that give materials their solid like characteristics to cause material flow. In other words, the material will not flow unless the applied stress exceeds a critical threshold value, typically referred to as the yield stress of that material; below this threshold the material deforms elastically and above it plastic deformation (*i.e.* flow) occurs. In regard to the material systems studied here, it means the ease with which the formulations can be extruded from the syringe of the printer when the force is applied through the plunger.

A stress ramp is one of the most commonly-used test methods to estimate the yield stress of materials, where the instantaneous viscosity of the sample is measured against an increasing applied shear stress. The shear stress corresponding to the peak viscosity (point of yield) is estimated as the yield stress of the sample. The (averaged) stress ramp data and measured shear viscosity of the formulations used to determine the yield stress of the formulations are presented in Fig. 7. The data acquisition was carried out in triplicate and each sample was only used once. The ramp duration was kept as 100 s for all formulations but to different final stress (from zero) in order to adequately capture the peak viscosity change and response beyond yielding.

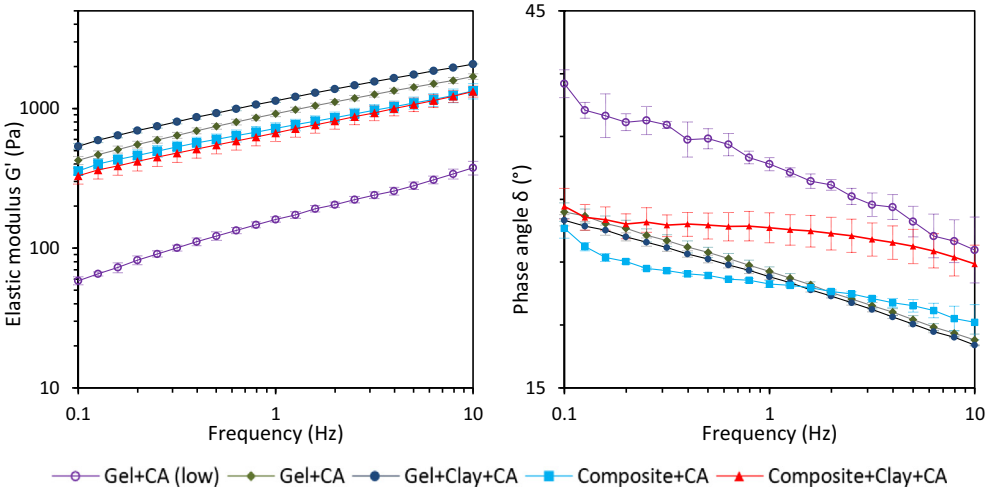

Fig. 5. Frequency sweep data showing elastic modulus (G′) (Log scale) and phase angle (δ) as a function of frequency.

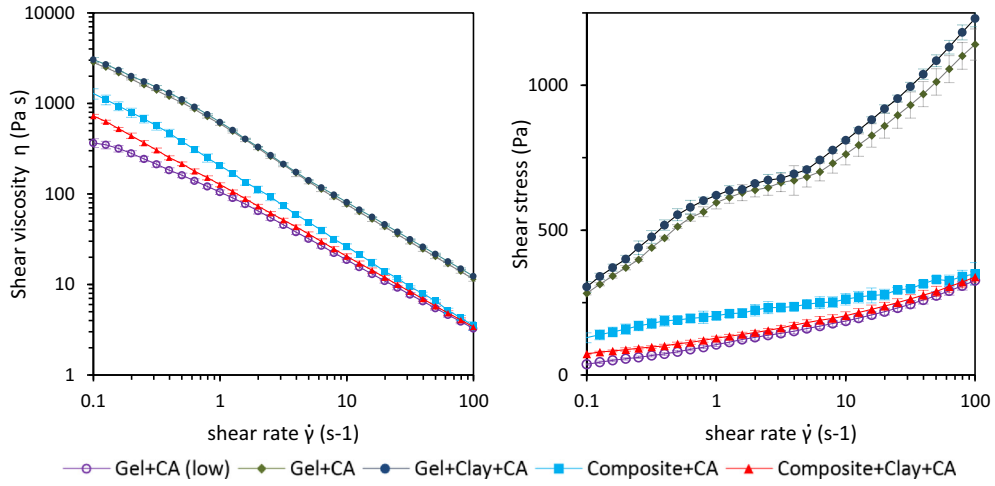

Fig. 6. Steady state shear viscosity (η) (Log scale) and shear stress (τ) as a function of shear rates.

The Gel + CA and Gel + Clay + CA samples were subjected to 0–300 Pa, whereas Composite + CA and Composite + Clay + CA samples were subjected to 0–200 Pa during the test. The error bars for viscosity have been omitted from Fig. 7 for clarity, with representative values reported in Table 3. Gel + CA (low) samples were omitted from the stress ramp test to estimate yield stress because the formulation was deemed too weak (low G′) to hold the extruded shape even though its low viscosity would make it easier to extrude through the syringe.

The yield stress for each of the formulations have been obtained from the shear stress value corresponding to the peak viscosity for each test run and is tabulated in Table 3. The data presented here is more reliable as they represent actual test data as opposed to results from the time averaged response plotted in Fig. 7. It is noted that the values presented in Table 3 cover the peak values presented in the plot thus confirming yield stress values are not affected by loading discrepancies. As expected Gel + CA and Gel + Clay + CA formulations have the highest yield stress and thus would be harder to extrude from the syringe compared to the other formulations with lower yield stress. The combined effect of clay and pulp fibres in facilitating easier flow is evident from the yield stress values.

3.8. 4D printing of cellulosic composites

The set-up of the printer and extruder is shown Fig. 8a. The print path, specimen dimensions are shown in Fig. 8b (blue: Composite + Clay + CA and red: Gel + CA) and the printed form is shown in Fig. 8c. This architecture has a programmed actuation pathway facilitated by means of the Gel + CA formulation around the base of petals. This petal design was chosen to take advantage of the programmed 'through-thickness strain mis-match' which is the driving force for transformations. The drying of the specimen at room temperature initiated the transformation (Fig. 8d) which was maximised by crosslinking fixing the new configuration as shown in Fig. 8e. The demonstration of the 3D printing of the responsive cellulose composite in the fabrication and actuation of a petal architecture is presented Fig. 8b–g.

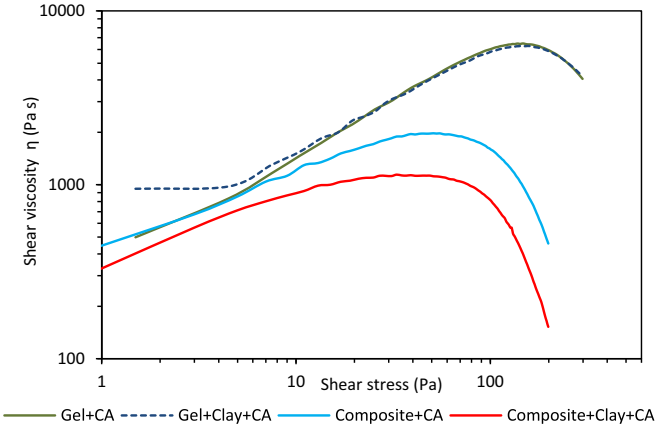

Fig. 7. Stress ramp plots showing yield stress of formulations at peak viscosity.

This new configuration is generated by virtue of greater strain differential achieved by means of enhanced dehydration of the materials at elevated temperatures. This transformed shape is deployed back to the flat configuration by placing in a water bath at room temperature - Fig. 8f. Upon drying, the petal architecture reverts to its 3D configuration as shown in Fig. 8g. The actuation between flat and 3D configuration is cyclic and can be repeated multiple times (>5) thus exhibiting shape memory behaviour. However, the extent of recovery after each cycle was not systematically characterised at this stage. The physical changes in cellulose fibres due to hydration and de-hydration cycles (*i.e.* hornification) and its influence on substrate porosity and thus on the actuation time has been studied for paper architectures [12]. Similarly, the same can be expected of the cyclic actuation of 3D printed cellulosic architectures albeit to a lesser extent due to the supporting hydrogel matrix adapting to the changes in fibres within the global form.

The example presented in Fig. 8 not only demonstrates the ability of the developed material system to be 3D printed but also its ability to morph out-of-plane by virtue of programmed strain mis-match *via* dehydration/hydration. It is envisaged that in conjunction with the versatility of additive layer manufacturing/3D printing methods, varying microstructures within an overall shape can be achieved and the responsive nature of material along with its tuneable parameters would result in hierarchical structures within a global form that can actuate in complex forms.

4. Conclusions

The development of a compliant composite cellulosic hydrogel integrating a high proportion of cellulosic material allowed use of a standard

Table 3
Yield stress for formulations.

Formulation	Peak viscosity (Pas)	Yield stress (Pa)
Gel + CA	7000 ± 800	140 ± 9
Gel + Clay + CA	6300 ± 380	147 ± 8
Composite + CA	2000 ± 290	46 ± 8
Composite + Clay + CA	1150 ± 230	38 ± 8

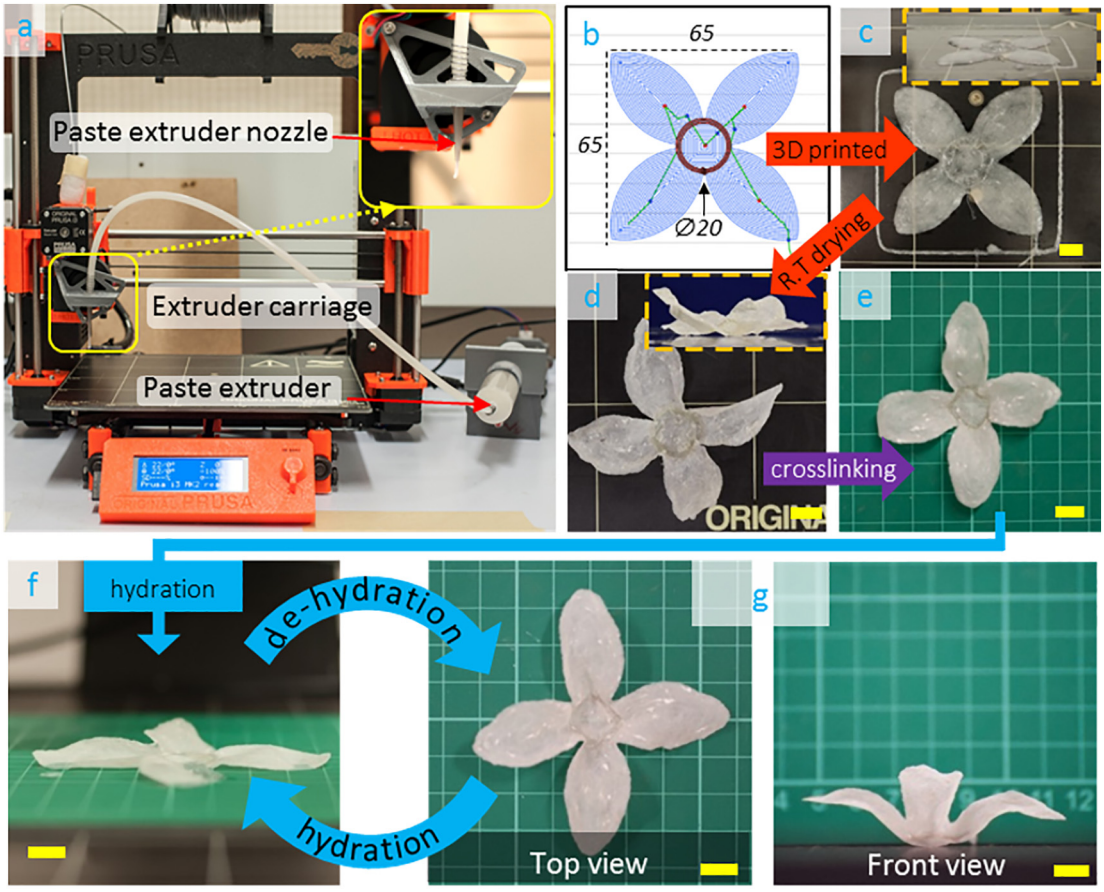

Fig. 8. (a) 3D printer and paste extruder set up; Extruder housing is shown in insert with the nozzle for printing gel and composite materials. (b–g) Fabrication of petal architecture (b) Generated print path from CAD model – dimensions are in mm (c) 3D printed form (d) Drying at room temperature initiating morphing (e) After crosslinking to maximise and fix the 3D shape (f) Deployed to flat configuration upon hydration (g) drying (dehydration) recovers the 3D petal shape. Side views are shown in insert. (Scale bar = 10 mm).

3D printer to control material placement without compromising the responsiveness of the cellulose to hydration. The addition of a cellulosic hydrogel overcame the issue of the frequent clogging of the print nozzle caused by shear thickening from the strong inherent hydrogen bonding between cellulose fibres, and allowed the composite to be extruded with precision. Dissociation of pulp fibres in the hydrogels not only imparted necessary shear thinning properties but also aided in the dissociation and distribution of pulp fibres through optimised mixing strategies. This directly resulted in the ability to use higher loading capacities of pulp fibres without clogging, allowing development of 3D printable cellulosic fibres. It was observed that permitting the crosslinking of these composites did not adversely affect the extrusion characteristics. Furthermore, it was imperative that the extruded/printed shapes produced are stable in an aqueous environment and do not disintegrate over the duration of the experiments. The choice of citric acid as a cross-linker enabled lower crosslinking temperatures (after printing of the shape) and an ecologically friendlier direction for further material development.

The rheological characterisation of the formulations containing citric acid confirmed that the samples were shear thinning which is essential for smooth and controlled extrusion in any syringe-based 3D printing extrusion process. The low critical strains for composite samples indicate that they flow readily when deformed, which is desirable. The yield stress characterisation enabled quantifiable measurement of the force required to extrude the formulations. These results enabled the selection process of the extruder system for the integration of this material system into the domain of 3D printing. The primary reason for the inclusion of the montmorillonite clay was to stabilise the formulations for long term storage, but an additional complementary effect on composite formulation was also noted. For example, traditionally, filler additions usually result in an increased solid like characteristics and viscosity thus hindering the material flow, but as demonstrated in the amplitude sweep and shear rate results, the combination of pulp and clay resulted in a more liquid like behaviour when deformed. The positive effect of clay-pulp interactions in lowering yield stress was also noted. It is believed that the intercalating clay platelets inhibit or even cleave hydrogen bonding between pulp, CMC and water when deformed. Further characterisation of the pulp-clay interaction and the microstructure in Composite + Clay + CA samples is required to confirm this hypothesis. However, the rheological characterisation of the samples confirms that the addition of clay improves the solid-like characteristics at rest and enhances the flow characteristics in formulations with pulp. These are ideal features for a 3D printing material as a liquid like behaviour (flow) is desired for ease of extrusion and solid like behaviour to hold the shape after extrusion (rest).

The swelling ratio of samples were determined after crosslinking to investigate the swelling potential of the samples as well as their aqueous stability. As expected, the citric acid formulations have considerably lower swelling potential when compared to self-crosslinked samples. However, it is paramount to generate controllable swelling without degrading the material. Additionally, the presence of crosslinking agent as opposed to self-crosslinking enables control over the extent of crosslinking which was found to influence the swelling potential. The role of the pulp network in restricting the swelling of the gel matrix was also noted. The formulations can be presumed to be stable throughout the hydration and dehydration cycles as the citric acid present in the formulations bridges to the cellulose backbone of CMC and pulp fibres after crosslinking. The amount of cross-linker (citric acid) used in the

formulations was obtained from previous literature studies and was kept constant as this was not a key parameter under investigation. Furthermore, the highly reactive nature of the intermediate (anhydride of citric acid) formed during the dehydration (crosslinking reaction) implies that all of the cross-linker will react with cellulose. However, it is crucial to investigate potential leaching of components following multiple cycles of hydration and de-hydration and its effect on shape memory. This will form part of the study investigating the stability of 4D printed forms and will be reported in future studies. The even dispersion of the ingredients within the composite and the pulp network should also prevent leaching out of clay particles from the crosslinked samples.

The adoption of pulp and cellulosic hydrogel in a composite form enabled integration of the cellulosic material into the domain of 3D printed materials without compromising its functionality while retaining the tuneable parameters such as varying microstructure porosity, temperature and fibre volume fraction. These parameters can be controlled to attain a programmable response from a global substrate through varying inherent 'through thickness strain mismatch' upon hydration/dehydration. The most distinguishable feature of the work presented here is the cellulosic content of the final material form. The cellulosic content for composite gels reported in relevant 4D printing literature varies from 0.8%–2.3 wt% of water content for MFC and NFC in hydrogel [19,28]. In the Composite + Clay + CA formulation, 2.5 wt% of cellulose fibres are present and an additional 2.5 wt% of CMC. This is indeed an intermediate state of the material formulated for processing (*i.e.* 3D printing). However, the final material state is a consolidated composite following drying and crosslinking which is devoid of water. The resulting composite is formulated to be 50% fibre and 50% CMC by weight. This strategy results in a greater fibre (reinforcement) content in the final printed form, and will enable designers to create bespoke architectures with varying microstructure for triggered morphing.

Implementation of 3D printing will not only ensure greater precision in the placement of materials but also facilitate the realisation of more complex architectures and actuation pathways for 4D printing. The printing parameters (*e.g.* nozzle diameter, print speed and orientation of reinforcements during printing process) and design choices (*e.g.* porosity and thickness) have significant influence on the morphing behaviour through guiding the strain gradient within the printed structure. Therefore, comprehensive understanding of how the process parameters and design choices can influence the morphing behaviour of printed architectures is essential to extract desired responses *i.e.* programmability. Presently, the authors are exploring and devising experimental procedures to determine the influence these parameters; this will be reported in a subsequent publication. The natural progression of the work presented here would be to control the inherent microstructure and final form through 3D printing by taking advantage of shear alignment of fibres. Realisation of specific 3D printed actuation pathways within a global architecture could lead to more complex actuation capable of sequential multi-stage deployment. The demonstration of a sustainable and cost-effective ink which is able to be used with commercial 3D printers is expected to encourage the widespread adoption of 4D printing. This should accelerate our understanding of the fundamental design principles by making 4D printing more accessible and attractive to a greater number of researchers.

Acknowledgements

MCM is supported by the Engineering and Physical Sciences Research Council through the EPSRC Centre for Doctoral Training in Advanced Composites for Innovation and Science [grant number EP/G036772/1], RST is supported by EPSRC Engineering Fellowships for Growth (grant number EP/M002489/1) and VPT is supported by an EPSRC Engineering Fellowship (EP/R01650X/1). The authors would also like to acknowledge Mr. Ed Aldred (School of Chemistry, University of Bristol) for his help in providing the training and facilitating the use of the rheometer. The Thinky Mixer was purchased thanks to a donation from Renee Bates Legacy Fund from the School of Physics, University of Bristol.

Data availability statement

All raw data reported in this paper is contained within the manuscript.

Author contributions

Manu C Mulakkal (Conceptualization; Data curation; Formal analysis; Investigation; Methodology; Project administration; Resources; Validation; Visualization; Roles/Writing - original draft; Writing - review & editing): MCM carried out the research, experiments and wrote the original manuscript. MCM also complied the revised manuscript in accordance with the reviewers suggestions.

Richard S Trask (Writing - review & editing): RST reviewed and made some additions to parts of the manuscript.

Valeska P Ting (Supervision, Writing – review & editing): VPT supervised the work regarding 4D printing, reviewed the full manuscript and made additions. VPT also reviewed and edited the revised manuscript.

Annela M Seddon (Supervision, Writing – review & editing): AMS supervised the work regarding developing hydrogel composite, reviewed the full manuscript and made additions.

References

[1] I. Burgert, P. Fratzl, Actuation systems in plants as prototypes for bioinspired devices, Philos. Transact. A Math. Phys. Eng. Sci. 367 (2009) 1541–1557, https://doi.org/10.1098/rsta.2009.0003.
[2] C. Dawson, J.F.V. Vincent, A.-M. Rocca, How pine cones open, Nature (London) 390 (1997) 668, https://doi.org/10.1038/37745.
[3] A.R. Studart, R.M. Erb, Bioinspired materials that self-shape through programmed microstructures, Soft Matter 10 (2014) 1284–1294, https://doi.org/10.1039/C3SM51883C.
[4] P.T. Martone, M. Boiler, I. Burgert, J. Dumais, J. Edwards, K. MacH, N. Rowe, M. Rueggeberg, R. Seidel, T. Speck, Mechanics without muscle: biomechanical inspiration from the plant world, Integr. Comp. Biol. 50 (2010) 888–907, https://doi.org/10.1093/icb/icq122.
[5] S. Kim, C. Laschi, B. Trimmer, Soft robotics: a bioinspired evolution in robotics, Trends Biotechnol. 31 (2013) 287–294, https://doi.org/10.1016/j.tibtech.2013.03.002.
[6] S. Schmitt, D.F.B. Haeufle, R. Blickhan, M. Günther, Nature as an engineer: one simple concept of a bio-inspired functional artificial muscle, Bioinspir. Biomim. 7 (2012), 36022. https://doi.org/10.1088/1748-3182/7/3/036022.
[7] S. Daynes, R.S. Trask, P.M. Weaver, Bio-inspired structural bistability employing elastomeric origami for morphing applications, Smart Mater. Struct. 23 (2014), 125011. https://doi.org/10.1088/0964-1726/23/12/125011.
[8] A.J. Braihi, Proposed cross-linking model for carboxymethyl cellulose/starch superabsorbent polymer blend, Int. J. Mater. Sci. Appl. 3 (2014) 363, https://doi.org/10.11648/j.ijmsa.20140306.23.
[9] J.R. Capadona, K. Shanmuganathan, D.J. Tyler, S.J. Rowan, C. Weder, Stimuli-responsive polymer nanocomposites inspired by the sea cucumber dermis, Science 319 (2008) 1370–1374, https://doi.org/10.1126/science.1153307.
[10] X. Chen, L. Mahadevan, A. Driks, O. Sahin, Bacillus spores as building blocks for stimuli-responsive materials and nanogenerators, Nat. Nanotechnol. 9 (2014) 137–141, https://doi.org/10.1038/nnano.2013.290.
[11] K. Oliver, A. Seddon, R.S. Trask, Morphing in nature and beyond: a review of natural and synthetic shape-changing materials and mechanisms, J. Mater. Sci. 51 (2016) 10663–10689, https://doi.org/10.1007/s10853-016-0295-8.
[12] M.C. Mulakkal, A.M. Seddon, G. Whittell, I. Manners, R.S. Trask, 4D fibrous materials: characterising the deployment of paper architectures, Smart Mater. Struct. 25 (2016), 95052. https://doi.org/10.1088/0964-1726/25/9/095052.
[13] K. Zhang, A. Geissler, M. Standhardt, S. Mehlhase, M. Gallei, L. Chen, C. Marie Thiele, Moisture-responsive films of cellulose stearoyl esters showing reversible shape transitions, Sci. Rep. 5 (2015), 11011. https://doi.org/10.1038/srep11011.
[14] Y. Habibi, L.A. Lucia, O.J. Rojas, Cellulose nanocrystals: chemistry, self-assembly, and applications, Chem. Rev. 110 (2010) 3479–3500, https://doi.org/10.1021/cr900339w.
[15] E. Reyssat, L. Mahadevan, How wet paper curls, EPL 93 (2011), 54001. https://doi.org/10.1209/0295-5075/93/54001.
[16] S. Tibbits, 4D printing: multi-material shape change, Archit. Des. 84 (2014) 116–121, https://doi.org/10.1002/ad.1710.
[17] H. Wei, Q. Zhang, Y. Yao, L. Liu, Y. Liu, J. Leng, Direct-write fabrication of 4D active shape-changing structures based on a shape memory polymer and its nanocomposite, ACS Appl. Mater. Interfaces 9 (2017) 876–883, https://doi.org/10.1021/acsami.6b12824.

[18] F. Momeni, S. M.Mehdi Hassani.N, X. Liu, J. Ni, A review of 4D printing, Mater. Des. 122 (2017) 42–79, https://doi.org/10.1016/j.matdes.2017.02.068.
[19] A. Sydney Gladman, E.A. Matsumoto, R.G. Nuzzo, L. Mahadevan, J.A. Lewis, Biomimetic 4D printing, Nat. Mater. (2016) 1–7, https://doi.org/10.1038/nmat4544.
[20] S.E. Bakarich, R. Gorkin, M. In Het Panhuis, G.M. Spinks, 4D printing with mechanically robust, thermally actuating hydrogels, Macromol. Rapid Commun. 36 (2015) 1211–1217, https://doi.org/10.1002/marc.201500079.
[21] E. Reyssat, L. Mahadevan, Hygromorphs: from pine cones to biomimetic bilayers, J. R. Soc. Interface 6 (2009) 951–957, https://doi.org/10.1098/rsif.2009.0184.
[22] M.A.S. Azizi Samir, F. Alloin, A. Dufresne, Review of recent research into cellulosic whiskers, their properties and their application in nanocomposite field, Biomacromolecules 6 (2005) 612–626, https://doi.org/10.1021/bm0493685.
[23] E. Malmström, A. Carlmark, Controlled grafting of cellulose fibres – an outlook beyond paper and cardboard, Polym. Chem. 3 (2012) 1702, https://doi.org/10.1039/c1py00445j.
[24] H. Kang, R. Liu, Y. Huang, Cellulose-based gels, Macromol. Chem. Phys. (2016) 1–13, https://doi.org/10.1002/macp.201500493.
[25] RSPro, Product Datasheet, WOOD, http://docs-europe.electrocomponents.com/webdocs/157c/0900766b8157cfcb.pdf 2017, Accessed date: 1 March 2017.
[26] COLORFABB, Product Datasheet, SPECIAL WOODFILL, https://www.goprint3d.co.uk/colorfabb-woodfill.html?keyword=&gclid=EAIaIQobChMImI68z7CQ1QIVZSjTCh2nOAk2EAQYAiABEgIz9fD_BwE 2017, Accessed date: 5 March 2017.
[27] K. Markstedt, J. Sundberg, P. Gatenholm, 3D Bioprinting of Cellulose Structures from an Ionic Liquid, 1, 3d Printing and Additive Manufacturing, 2014 115–121, https://doi.org/10.1089/3dp.2014.0004.
[28] K. Markstedt, A. Mantas, I. Tournier, H. Martínez Ávila, D. Hägg, P. Gatenholm, 3D bioprinting human chondrocytes with nanocellulose-alginate bioink for cartilage tissue engineering applications, Biomacromolecules 16 (2015) 1489–1496, https://doi.org/10.1021/acs.biomac.5b00188.
[29] K.M.O. Håkansson, I.C. Henriksson, C. de la Peña Vázquez, V. Kuzmenko, K. Markstedt, P. Enoksson, P. Gatenholm, Solidification of 3D printed nanofibril hydrogels into functional 3D cellulose structures, Adv. Mater. Technol. 1 (2016) https://doi.org/10.1002/admt.201600096 (1600096–n/a).
[30] P. Kärki, H. Orelma, V. Klar, 3D-printing of Cellulose-based Materials – Cellulose From Finland.fi, http://cellulosefromfinland.fi/3d-printing-of-cellulose-based-materials/ 2016, Accessed date: 1 March 2017.
[31] J. Leppiniemi, P. Lahtinen, A. Paajanen, R. Mahlberg, S. Metsä-Kortelainen, T. Pinomaa, H. Pajari, I. Vikholm-Lundin, P. Pursula, V.P. Hytönen, 3D-printable bioactivated nanocellulose-alginate hydrogels, ACS Appl. Mater. Interfaces 9 (2017) 21959–21970, https://doi.org/10.1021/acsami.7b02756.
[32] R. Jones, P. Haufe, E. Sells, P. Iravani, V. Olliver, C. Palmer, A. Bowyer, Reprap - the replicating rapid prototyper, Robotica 29 (2011) 177–191, https://doi.org/10.1017/S026357471000069X.
[33] E. De Bruijn, On the Viability of the Open Source Development Model for the Design of Physical Objec, Lessons Learned From the RepRap Project, 2010https://doi.org/10.1002/cbdv.200490137/abstract\nhttp://scholar.google.com/scholar?hl=en.
[34] C. Chang, L. Zhang, Cellulose-based hydrogels: present status and application prospects, Carbohydr. Polym. 84 (2011) 40–53, https://doi.org/10.1016/j.carbpol.2010.12.023.
[35] W.J. Zheng, J. Gao, Z. Wei, J. Zhou, Y.M. Chen, Facile fabrication of self-healing carboxymethyl cellulose hydrogels, Eur. Polym. J. 72 (2015) 514–522, https://doi.org/10.1016/j.eurpolymj.2015.06.013.
[36] A. Sczostak, Cotton linters: an alternative cellulosic raw material, Macromol. Symp. 280 (2009) 45–53, https://doi.org/10.1002/masy.200950606.
[37] K. Borůvková, J. Wiener, S. Kukreja, Thermal self cross-linking of carboxymethylcellulose, Acad. Coord. Cent. J. XVIII (2012) 6–13.
[38] S. Spoljaric, A. Salminen, N.D. Luong, J. Seppälä, Crosslinked nanofibrillated cellulose: poly(acrylic acid) nanocomposite films; enhanced mechanical performance in aqueous environments, Cellulose 20 (2013) 2991–3005, https://doi.org/10.1007/s10570-013-0061-x.
[39] J.P. Cook, G.W. Goodall, O.V. Khutoryanskaya, V.V. Khutoryanskiy, Microwave-assisted hydrogel synthesis: a new method for crosslinking polymers in aqueous solutions, Macromol. Rapid Commun. 33 (2012) 332–336, https://doi.org/10.1002/marc.201100742.
[40] C. Demitri, R. Del Sole, F. Scalera, A. Sannino, G. Vasapollo, A. Maffezzoli, L. Ambrosio, L. Nicolais, Novel superabsorbent cellulose-based hydrogels crosslinked with citric acid, J. Appl. Polym. Sci. 110 (2008) 2453–2460, https://doi.org/10.1002/app.28660.
[41] M. Hashem, S. Sharaf, M.M. Abd El-Hady, A. Hebeish, Synthesis and characterization of novel carboxymethylcellulose hydrogels and carboxymethylcellulolse-hydrogel-ZnO-nanocomposites, Carbohydr. Polym. 95 (2013) 421–427, https://doi.org/10.1016/j.carbpol.2013.03.013.
[42] J.M. Zuidema, C.J. Rivet, R.J. Gilbert, F.A. Morrison, A protocol for rheological characterization of hydrogels for tissue engineering strategies, J Biomed Mater Res B Appl Biomater 102 (2014) 1063–1073, https://doi.org/10.1002/jbm.b.33088.
[43] Malvern, Evaluating the Rheological Properties of Hyaluronic Acid Hydrogels for Dermal Filler Applications, http://www.malvern.com/en/support/resource-center/application-notes/AN150112-prop-HA-hydrogels-Dermal-Filler.aspx 2016.
[44] O. Levinger, Syringe Extruder, http://www.instructables.com/id/Syringe-Extruder/ 2015, Accessed date: 22 December 2017.
[45] K.P. Menard, Dynamic Mechanical Analysis: A Pratical Introduction, CRC-Press, 1999.
[46] W.A. White, E. Pichler, Water-sorption characteristics of clay minerals, Illinois State Geol. Surv. 266 (1959) (20 p).